

Optimizing the optical array geometry for TRIDENT

Qichao Chang,^{a,*} Fan Hu,^b Iwan Morton-Blake^c and Donglian Xu^{a,c} for the TRIDENT collaboration

^a*School of Physics and Astronomy, Shanghai Jiao Tong Univeristy, 800 Dongchuan Rd, Shanghai, China*

^b*Department of Astronomy, Peking University, 5 Yiheyuan Rd, Beijing, China*

^c*Tsung-Dao Lee Institute, Shanghai Jiao Tong Univeristy, 520 Shengrong Rd, Shanghai, China*

E-mail: chang55363@sjtu.edu.cn

The observation of astrophysical neutrino sources provides smoking-gun evidence for the origin of cosmic rays. IceCube has recently reported an excess of neutrino flux from NGC 1068 with a significance of 4.2σ . TRIDENT is a proposed next-generation neutrino telescope located in the South China Sea. Owing to its large size, novel detector design, and location near the equator, TRIDENT will provide outstanding sensitivity to neutrino sources over the entire sky. In order to evaluate the detector's performance, we have conducted simulation studies using track-like events. Here, we present the effective area and angular resolution of TRIDENT, based on the optimization of the Penrose tilling layout where the spacing is optimized. Other array layout options such as Sunflower and Cluster, are also compared in terms of point source sensitivity using up-going track-like neutrino events. Finally, we will also briefly introduce the pilot TRIDENT Phase-I project.

38th International Cosmic Ray Conference (ICRC2023)
26 July - 3 August, 2023
Nagoya, Japan



*Speaker

1. Introduction

IceCube has recently identified NGC 1068 as a new potential celestial neutrino source with a significance of 4.2σ [1]. This discovery underscores the necessity of next generation neutrino telescopes with excellent angular resolution and effective area.

TRIDENT (TRopIcal DEep-sea Neutrino Telescope) is a newly proposed next-generation neutrino telescope at the South China Sea, with a projected monitoring volume of approximately 7.5 km^3 and the location near the equator [2]. TRIDENT consists of ~ 1200 strings that make up the Penrose tiling distribution having the relatively sparse and dense string arrangement, as shown in Fig. 1. Each string contains 20 hybrid Digital Optical Modules (hDOMs) of Photomultiplier Tubes (PMTs) for high photon collection efficiency and small Silicon Photomultiplier (SiPM) arrays for precise timing resolution [3]. With the unique optical array of non-uniform geometry, TRIDENT will exhibit better detection performance in searching for astrophysical neutrino sources over the whole sky to study extreme cosmic environments through neutrino messengers.

In September 2021, the TRIDENT Pathfinder team conducted its first expedition to the South China Sea [2]. During this expedition, the team successfully deployed several sets of self-developed experimental instruments in the predetermined site, and the results proved that the geographical location and environment of the selected location are suitable for instrumenting a neutrino telescope. The measured optical properties of seawater will serve as critical parameters in the following simulation.

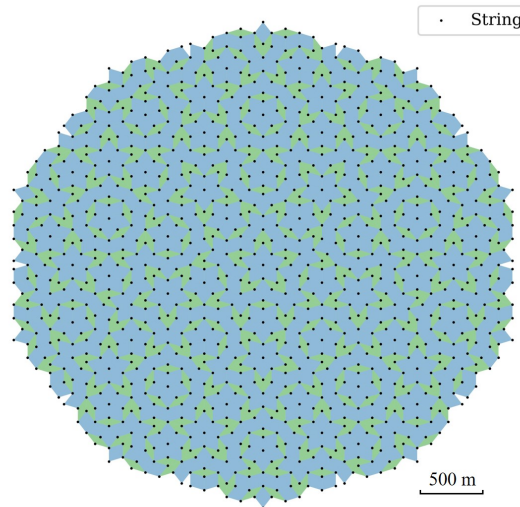


Figure 1: Geometry layout of the TRIDENT array following a Penrose tiling distribution. The green zone represents the string spacing ~ 70 m, and the blue zone ~ 110 m.

In these proceedings, we present current results on optimizing the optical array geometry for TRIDENT. We adjust the spacing among the strings and investigate its impact on the detector's effective area and angular resolution. We also conduct a comparative analysis of the Penrose tiling layout with alternative configurations such as the Sunflower and Cluster. Finally, we briefly outline the performance of the pilot TRIDENT Phase-I array which comprised of 10 strings.

2. Simulation Setup

A neutrino telescope can detect neutrinos of all flavors via the Cherenkov light produced by the neutrino-induced secondary charged particles. This work focuses on the muon neutrino charged current (CC) interaction channel since muon neutrinos with sub-degree angular resolution are considered as the preferred events to evaluate the point source-searching sensitivities.

The TRIDENT simulation pipeline integrates two main components to accurately simulate neutrino interactions and detector responses. The neutrino generator incorporates CORSIKA8 [4] to provide information on secondary particles resulting from the Deep-Inelastic Scattering (DIS) vertex and subsequent muons. Meanwhile, Geant4 [5] is employed to simulate the propagation of charged particles and the emission of Cherenkov photons in seawater. The propagation of optical photons is specifically handled by OptiX [6], which utilizes GPU acceleration. Lastly, the process by which photons reach the hDOMs is simulated in Geant4.

In CORSIKA8, the TRIDENT detector is represented as a cylinder with a radius of 2200 m and a height of 800 m, situated 2900 m below sea level. Neutrinos are sampled within an energy range of 1 TeV to 100 TeV with an energy spectral index of -1.1, and their directions are uniformly sampled within a 4π solid angle. Furthermore, the simulation incorporates relevant physical processes and models, including the lepton-hadron response model in PYTHIA-8.3 [7]. The neutrino Deep Inelastic Scattering (DIS) process is managed in CORSIKA8, resulting in the production of secondary particles that serve as inputs for Geant4.

In Geant4, the TRIDENT detector is constructed with approximately 1200 strings, each carrying 20 hDOMs. The geometry is a cylinder whose radius and height are 400 m larger than the optical array, and filled with water, implementing the optical properties measured from TRIDENT Pathfinder above. This configuration simulates the propagation of charged secondary particles and generates Cherenkov photons. The OptiX ray-traced framework is employed to propagate these photons to hDOMs. The position of a photon is recorded once it reaches a hDOM's surface. Subsequently, the Cherenkov photons reach the PMTs and SiPMs situated within the detectors, with the precise arrival times of each photon being recorded. By analyzing the hit times and locations of these photons, the detection performance of TRIDENT can be assessed.

3. TRIDENT full strings with varying spacing

As shown in Fig. 1, the Penrose layout of TRIDENT assumes the shape of a flat cake with about the 3:1 ratio of its total radius and height, to lessen the potential of long string entanglements. Compared with other neutrino telescopes, TRIDENT will have a larger number of strings, larger volume in seawater and unique array geometry. To further improve the potential performance of TRIDENT, we would like to understand how different string spacings would affect the effective area and angular resolution. Here, we modified the total radius of the Penrose layout, which means the distance from the outermost string of the array to the center, to evaluate its effective area and angular resolution. Notably, the different total radii represent that all string spacings in the Penrose layout are scaled up or down in equal proportions.

3.1 Effective Area

The effective area is a key parameter to quantify the efficiency of a neutrino telescope in detecting neutrino events. Assuming the considered neutrino physical flux is $F_{\text{phy}}(\hat{n}, E)$, the effective area $A_{\text{eff}}(\hat{n}, E)$ is defined as the following equation:

$$A_{\text{eff}}(\hat{n}, E) \equiv \frac{dN}{dt \, dn \, dE}(\hat{n}, E) / F_{\text{phy}}(\hat{n}, E) \quad (1)$$

where $\frac{dN}{dt \, dn \, dE}(E, \hat{n})$ represents the number of events that can be observed by the detector per unit of energy and solid angle at the energy E and direction \hat{n} .

Before any further analysis, the event selection needs to be performed once we have done the detector simulation. In this study, we have set the selection criterion for the simulated neutrino events as the following:

1. The total number of photons detected by PMTs and SiPMs is not less than 15.
2. The detected photons should be distributed on at least 2 strings on the array.

Such criteria allow us to select bright neutrino events that are less influenced by dark noise of PMTs and SiPMs, as well as optical backgrounds from Potassium-40 decay. The event selection also aids in filtering out events that are challenging for the reconstruction algorithm to handle.

By dividing the simulated events into different direction and energy bins and counting the number of observed events in each bin, the effective area can be evaluated as the following equation:

$$A_{\text{eff}}(\hat{n}, E) = \frac{1}{N \Delta E \Delta \Omega} \sum_i^{N_{\text{bin}}} [I_{\text{sel}}(i) \times w_i] \quad (2)$$

where $\sum_i^{N_{\text{bin}}}$ means summing events that belong to the interval of the given energy and solid angle, N_{bin} is the number of events in the interval, $\Delta E \Delta \Omega$ represents the phase space size of the interval. I_{sel} indicates whether or not an event has passed the selection criteria. w_i is the weighting term that incorporates the importance sampling of injected neutrino events, which also includes the interaction probability of neutrinos around the detector and the Earth absorption effect. In addition, w_i represents weights at the time of sampling which is related to the probability of the neutrino reaction and muon propagation, and $I_{\text{sel}}(i)$ relies on the detector's ability and the condition of event selection.

Taking varying total radii of the Penrose layout, the effective area as a function of the neutrino energy with only up-going neutrino events (the zenith angle of neutrinos is larger than 90°) is shown in Fig. 2, where only 3 typical total radii 1000 m, 2000 m and 3000 m are displayed. As the neutrino energy increases, the effective area of different total radii also gradually increases in logarithmic coordinate systems. The figure also shows the larger the total radius of the Penrose layout, the larger the effective area of the detector. Particularly, the effective area at the neutrino energy of around 100 TeV is respectively about $4 \times 10^2 \text{ m}^2$, $1 \times 10^3 \text{ m}^2$ and $2 \times 10^3 \text{ m}^2$ with the total radius of 1000 m, 2000 m and 3000 m. Nevertheless, when the neutrino energy is around 1 TeV, the effective area with the total radius of both 3000 m and 2000 m is almost the same, and is about 2 times larger than 1000 m. This result primarily arises from the fact that the events meeting selection criteria with the total radius of 3000 m are fewer compared to those with the radius of 2000 m, despite the larger volume encompassed by the 3000 m radius.

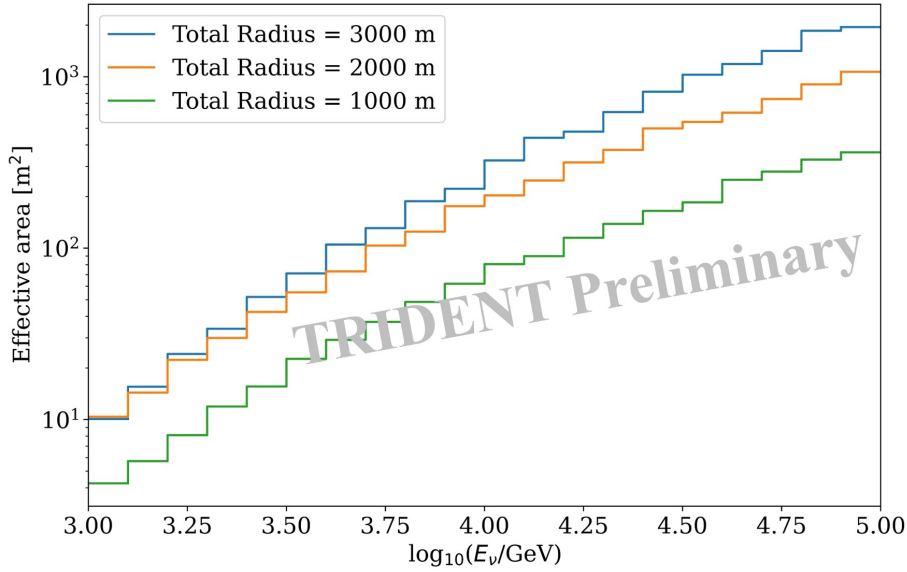


Figure 2: The effective area as a function of the primary neutrino energy for ν_μ with only up-going events. The blue, orange and green curves represent the total radius of 3000 m, 2000 m and 1000 m, respectively.

3.2 Angular Resolution

The reconstruction algorithm and process of muon neutrino events are consistent with those described in paper [2], where the M-estimator maximum likelihood function and the Single-Photon-Electron (SPE) maximum likelihood method are used to reconstruct the track of muons. The angular resolution as a function of the neutrino energy is shown in Fig. 3, where muon neutrino events in all directions are taken into account. As the total radius decreases, the angular resolution gradually becomes better. Especially for 1000 m and 2000 m, the angular error is expected to reach 0.1° or lower at the neutrino energy of around 100 TeV, which has reached the top level of neutrino telescopes in the world. On account of the large string spacing, the detector with the total radius of 3000 m will only receive a relatively small number of photons, which is detrimental to track reconstruction, and the angular resolution is much worse.

Furthermore, the angular resolution with only vertical neutrinos or horizontal neutrinos is also considered, which means the absolute value of the cosine of the neutrino zenith angle is larger or smaller than 0.5. The results show the angular resolution for vertical neutrinos becomes better as the total radius decreases, but for horizontal neutrinos, the angular resolution hardly changes with the total radius. This is due to the obvious difference in the radius and height of the detector.

4. Compare with Other Geometry Layouts

Apart from the Penrose layout, the Sunflower and Cluster layouts are also considered, each with the same number of configured strings. For the Sunflower layout, it expands to a total radius of 2000 m, distributed in equal proportions as described in paper [8], with a vertical spacing of 30 m among hDOMs. The Cluster layout exhibits several small clusters distributed in a manner analogous to the Sunflower layout, spanning a total radius of 2000 m. Each small cluster comprises

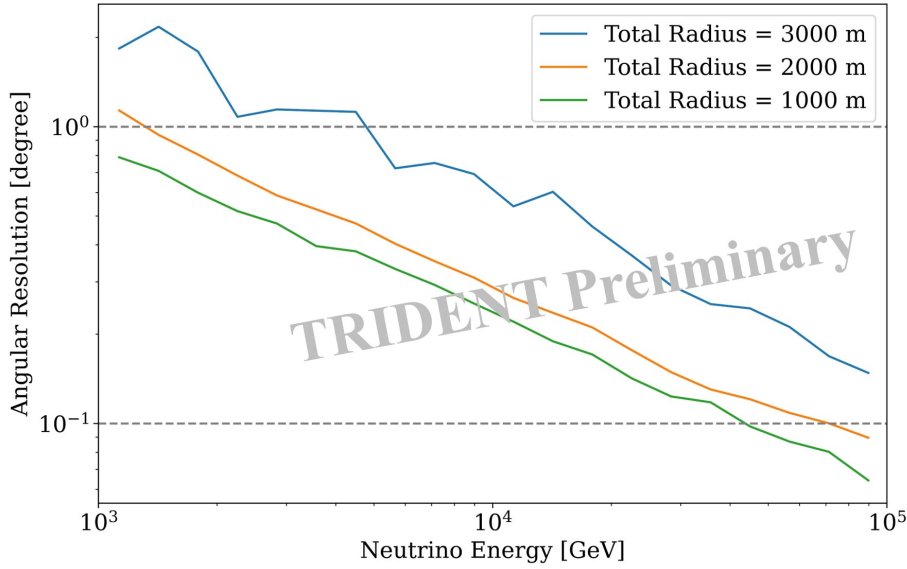


Figure 3: The median of angular error as a function of the primary neutrino energy for ν_μ track events. The blue, orange and green curves represent the total radius of 3000 m, 2000 m and 1000 m, respectively.

seven strings, with one centrally located and the remainder evenly dispersed on a circle with an approximate radius of 50 m.

With the different layouts in mind, a comprehensive simulation for TRIDENT’s performance is carried out using only up-going muon neutrino events. This method allows us to explore the sensitivity to astrophysical neutrino sources from all directions across the sky, as depicted in Fig. 4. In these simulations, the telescope’s observation time is set at ten years.

We assume an energy spectral index of -3 for neutrinos emanating from astrophysical sources and set a detection threshold of 1 TeV. Consequently, we can calculate the necessary flux from various astrophysical neutrino sources at distinct declinations to meet the selection criteria. This approach facilitates the detection of signals with a confidence level of 5σ .

Both the Penrose tiling and Sunflower layouts, each with a total radius of 2000 m, demonstrate excellent potential for discovering astrophysical neutrino sources over a data collection period of 10 years, outperforming the Cluster layout. The Sunflower layout offers sensitivity nearly on par with the Penrose layout across the entire sky. Notably, all these arrays yield the highest sensitivity near the South Pole ($\sin(\delta) \sim -1$) for the detection of muon neutrinos.

5. TRIDENT Phase-1

After the successful completion of the TRIDENT pathfinder experiment, a pilot project, TRIDENT Phase-I with 10 strings is scheduled. Expected to starting commissioning around 2026, TRIDENT Phase-I will become the first neutrino telescope near the equator, thus adding unique sky coverage to the global neutrino astronomy network. This work will also serve as a validation of the novel techniques implemented in TRIDENT, such as the hDOM.

The array arrangement of 10 strings in TRIDENT Phase-I will be optimized for track events, as shown in Fig. 5. Using the same simulation and analysis methods introduced above, we found that a

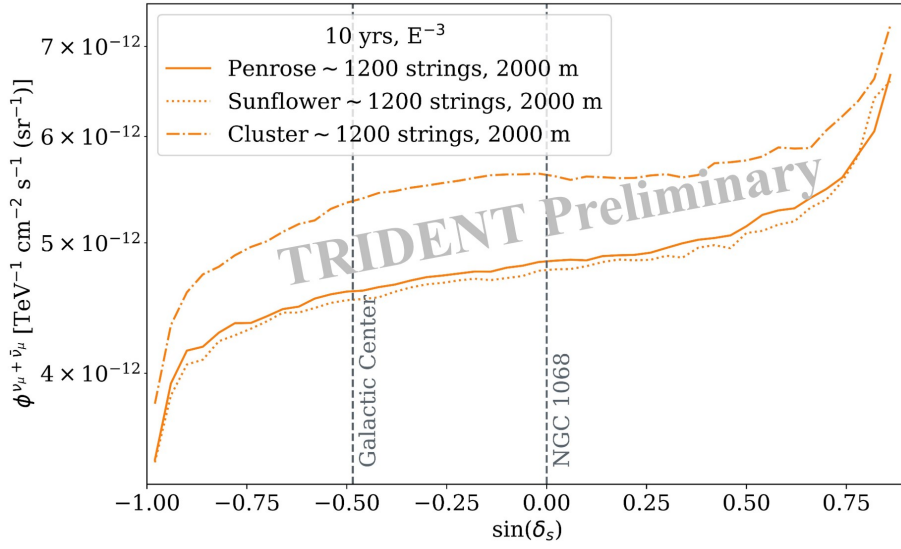


Figure 4: All sky point source 5σ discovery potential for Penrose (solid line), Sunflower (dotted line) and Cluster (dashed line) layout with 10 years of data taking, which is corresponded to a source spectrum index of 3 and minimum energy of 1 TeV. The x axis represents the sine declination. All these layouts have ~ 1200 strings, and both Sunflower and Cluster layouts have the total radius of 2000 m.

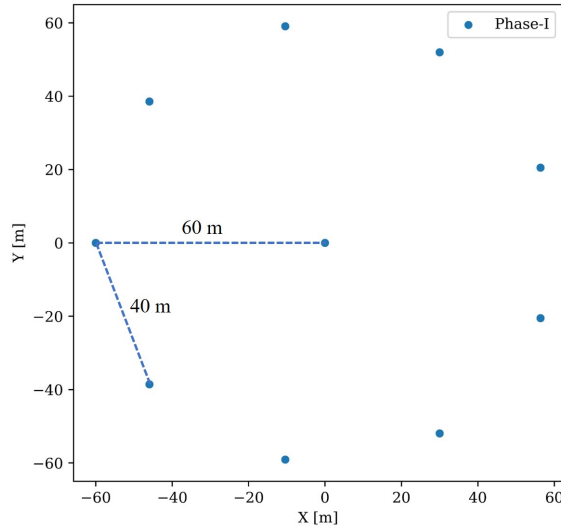


Figure 5: Geometry layout of the TRIDENT Phase-1 array.

vertical spacing between hDOMs of 40 m and a horizontal spacing between strings of 60 m suits for the purpose of TRIDENT Phase-1. In such geometry configuration, we found the median of angular resolution for muon neutrino events was 1.3° , and the effective area reached to 1.3 m^2 at energy of 10 TeV. Given the flux of atmospheric neutrinos [9] measured by IceCube, TRIDENT Phase-1 will detect about 300 atmospheric muon neutrino events per year, providing enough statistics for verifying the performance of the detector.

6. Summary and Outlook

In this work, we have explored the performance of TRIDENT, which utilizes the Penrose geometry as its array layout. To study its detection efficiency, we sampled muon neutrinos with the energy ranging from 1 TeV to 100 TeV and performed full event simulation. We calculated the effective area and the angular resolution of the detector for muon neutrinos with varying array total radii. We found the effective area will increase while the angular resolution gets worse as the total radius increases. A good detector sensitivity to neutrino sources depends on both the effective area and the angular resolution. The optimization of the string spacing is still under evaluation. Besides, for cascade events like ν_e [10] and ν_τ [11], the detection performance of TRIDENT should also be considered to further optimize the optical array geometry.

Apart from the string spacing of the Penrose layout, we have also studied the influence of the string geometry layout. We evaluated and compared the all-sky point source 5σ discovery potential with 10 years of data taking time for the Penrose, Sunflower, and Cluster layouts, respectively. The result shows the Penrose and Sunflower layouts have similar sensitivities, which are better than the Cluster layout.

In addition, we evaluated the performance of the TRIDENT Phase-I array. With instrumented 10 strings, TRIDENT Phase-I is expected to have an angular resolution of about 1.3° at energy of 10 TeV and can detect about 300 atmospheric muon neutrino events per year.

In the future, we plan to simulate higher energy muon neutrino events with larger number of samples. Meanwhile, the background generated from PMTs, SiPMs, Potassium-40 and bioluminescence in seawater will be added to inspect the reconstruction algorithm for muon neutrino events.

References

- [1] **IceCube** Collaboration, Abbasi, R. et al., *Science* **378** (2022) 538–543.
- [2] Z. P. Ye et al., “Proposal for a neutrino telescope in South China Sea”, arXiv:2207.04519.
- [3] F. Hu, Z. Li, and D. Xu, PoS(ICRC2021)1043 (2021).
- [4] **CORSIKA8** Collaboration, R. Ulrich et al., PoS(ICRC2021)474 (2021).
- [5] J. Allison et al., *IEEE Trans. Nucl. Sci.* **53** (2006) 270.
- [6] S. Blyth, *EPJ Web Conf.* **214** (2019) 02027.
- [7] C. Bierlich et al., arXiv:2203.11601.
- [8] **IceCube-Gen2** Collaboration, V. Basu et al., arXiv:2107.08837.
- [9] Aartsen, M.G. et al., *Astrophys. J.* **833** (1), 3
- [10] F Zhang et al., PoS(ICRC2023)1207 (these proceedings).
- [11] T Wei et al., PoS(ICRC2023)1092 (these proceedings).